Atmos. Chem. Phys., 9, 7289–7301, 2009
www.atmos-chem-phys.net/9/7289/2009/
© Author(s) 2009. This work is distributed under
the Creative Commons Attribution 3.0 License.

Atmospheric Chemistry and Physics

Ship emitted NO_2 in the Indian Ocean: comparison of model results with satellite data

K. Franke[1,2], **A. Richter**[1], **H. Bovensmann**[1], **V. Eyring**[2], **P. Jöckel**[3], **P. Hoor**[3], **and J. P. Burrows**[1,4]

[1]University of Bremen, Institute for Environmental Physics, Bremen, Germany
[2]Deutsches Zentrum für Luft- und Raumfahrt, Institut für Physik der Atmosphäre, Oberpfaffenhofen, Germany
[3]Max Planck Institute for Chemistry, Mainz, Germany
[4]Centre for Ecology and Hydrology, Wallingford, UK

Received: 25 July 2008 – Published in Atmos. Chem. Phys. Discuss.: 21 August 2008
Revised: 2 September 2009 – Accepted: 11 September 2009 – Published: 1 October 2009

Abstract. The inventory of NO_x emission from international shipping has been evaluated by comparing NO_2 tropospheric columns derived from the satellite instruments SCIAMACHY (January 2003 to February 2008), GOME (January 1996 to June 2003), and GOME-2 (March 2007 to February 2008) to NO_2 columns calculated with the atmospheric chemistry general circulation model ECHAM5/MESSy1 (January 2000 to October 2005). For both measurements and model consistently the tropospheric excess method was used to obtain mean NO_2 columns over the shipping lane from India to Indonesia, and over two ship free regions, the Bay of Bengal and the central Indian Ocean. The long-term data set from SCIAMACHY yields the first monthly analysis of ship induced NO_2 enhancements in the Indian Ocean. Comparison of data from the three instruments and in addition OMI reveals differences between the datasets which are discussed with respect to the diurnal cycle of NO_2 and the increase in shipping traffic over the time period studied.

In general, the model simulates the differences between the regions affected by ship pollution and ship free regions reasonably well. Minor discrepancies between model results and satellite data were identified during biomass burning seasons in March to May over India and the Indochinese Peninsula and August to October over Indonesia. We conclude that the NO_x ship emission inventory used in this study is a good approximation of NO_x ship emissions in the Indian Ocean for the years 2002 to 2007. It assumes that around $6\,\mathrm{Tg(N)\,yr^{-1}}$ are emitted by international shipping globally, resulting in $90\,\mathrm{Gg(N)\,yr^{-1}}$ in the region of interest when using Automated Mutual Assistance Vessel Rescue System (AMVER) as spatial proxy. A second model run using lower ship emissions estimates of 3–4 $\mathrm{Tg(N)\,yr^{-1}}$ globally results in poorer agreement with the satellite data.

Correspondence to: A. Richter
(andreas.richter@iup.physik.uni-bremen.de)

1 Introduction

Since the industrial revolution the amount of freight transported by international shipping has continually increased. Being powered by fossil fuel, ships contribute to the anthropogenic burden of air pollutants. One important pollutant emitted by ships is nitrogen monoxide (NO). In the atmosphere NO reacts with ozone (O_3) to form nitrogen dioxide (NO_2). The sum of NO and NO_2, which is known as NO_x, is pseudo conserved. As NO_x participates in the catalytic production of tropospheric ozone, accurate knowledge of the amount and distribution of NO_x is needed to understand and assess the role of ship emissions on tropospheric composition and climate. Recent estimates of the global NO_x emissions from international shipping vary over a large range. The global emission data base EDGAR3.2 includes data for 1995 (Olivier and Berdowsky, 2001), which if scaled to year 2000 values assuming a growth rate of $1.5\%\,\mathrm{yr^{-1}}$, results in annual NO_x emissions of 3.1 Tg(N), similar to the emission totals published by Corbett et al. (1999) and Endresen et al. (2003). Later estimates vary from $5.9\,\mathrm{Tg(N)\,yr^{-1}}$ (Corbett and Koehler, 2003) to $6.4\,\mathrm{Tg(N)\,yr^{-1}}$ (Eyring et al., 2005) for the year 2000 which are similar to recent estimates of the

Published by Copernicus Publications on behalf of the European Geosciences Union.

International Maritime Organization (IMO) greenhouse gas study (Buhaug et al., 2009). In addition to uncertainties in global emission totals, the knowledge of the spatial distribution is limited. As pointed out by Wang et al. (2008), ship activity patterns estimated by the International Comprehensive Ocean-Atmosphere Data Set (ICOADS) and the Automated Mutual-assistance Vessel Rescue System (AMVER) data set have different spatial and statistical sampling biases. Using these or similar NO_x shipping inventories, models have simulated and investigated the impact of shipping emission on tropospheric ozone (Lawrence and Crutzen, 1999; Kasibhatla et al., 2000; Eyring et al., 2007). Using the EDGAR3.2 dataset, the study by Eyring et al. (2007) shows maximum contributions from shipping to annual mean near-surface O_3 occur over the North Atlantic (5–6 ppbv in 2000).

Ship emissions of NO_x have been detected in the marine boundary layer (MBL) in satellite data (Richter et al., 2004; Beirle et al., 2004). These studies showed that the NO_2 enhancement in the shipping lane in the north-eastern Indian Ocean and the Red Sea is unambiguously identified from space. To estimate an emission rate from the satellite NO_2, it is necessary to estimate the lifetime of NO_x. For this purpose, Richter et al. (2004) used OH concentrations calculated by Song et al. (2003) to estimate a lifetime of 5.6 h, whereas Beirle et al. (2004) deduced a mean lifetime of about 1.9–6.0 h from seasonal changes in the pollutant distribution. Both studies concluded that reasonable agreement exists between the estimate of emissions made using satellite data and that available from emission inventories. However, it is clear that the estimation of lifetime of NO_x is one significant source of uncertainty in this comparison.

An alternative approach to investigate the consistency of emission inventories with NO_2 measurements is to calculate the column or concentration of NO_x levels with atmospheric chemistry models. Kasibhatla et al. (2000) and Davis et al. (2001) used ship emission totals of $3\,\mathrm{Tg(N)\,yr^{-1}}$ in global chemistry models and compared them to airborne measurements. They conclude that there is an overestimation of ship induced NO_x in the models and attribute this to the coarse resolution of the models and the uncertainties in the inventories. Eyring et al. (2007) compared the model output of eight global models at the local time of SCIAMACHY overpass to the satellite data of Richter et al. (2004). Although the geographical pattern of tropospheric NO_2 is well reproduced, modelled values of the tropospheric column are higher than those observed by SCIAMACHY over the ocean. The shipping lane in the Indian Ocean is not resolved in these simulations because of the low horizontal resolution in the models (between $5.6^\circ \times 5.6^\circ$ and $2.8^\circ \times 2.8^\circ$) compared to the satellite data ($30 \times 60\,\mathrm{km^2}$, i.e. $0.27^\circ \times 0.54^\circ$ at the equator). The study also compares the NO_2 total tropospheric columns to the SCIAMACHY observations without applying the tropospheric excess method to the model output. It has been shown by Lauer et al. (2002) that these two quantities differ.

The goal of this work is a quantitative assessment of the various NO_x ship emission estimates that have been published so far. This is achieved by comparing an extended set of satellite NO_2 data with results of the atmospheric chemistry general circulation model ECHAM5/MESSy1. In order to have a consistent comparison of modeled and measured NO_2 columns, the NO_2 tropospheric excess column has been generated from modelled and measured data sets for the first time in the context of ship emissions. Additionally, satellite data is rescaled to match the coarser resolution of the model. In this manner sources of systematic bias in the two data sets of tropospheric column NO_2 were minimised. Subsequently the behaviour and magnitude of these columns are analysed and the consistency of the emission inventories for the Indian Ocean with the satellite measurements is investigated.

2 Data retrieval and analysis

2.1 Tropospheric NO_2 columns retrieved from space

The tropospheric NO_2 columns are retrieved from measurements of the upwelling solar radiation in nadir viewing geometry by the three spectrometers GOME (Burrows et al., 1999; Richter and Burrows, 2002), SCIAMACHY (Burrows et al., 1995; Bovensmann et al., 1999; Richter et al., 2004), and GOME-2 (Callies et al., 2000), which fly on board the satellites ERS-2, ENVISAT, and METOP-A, respectively. These satellites are in sun synchronous orbits having equator crossing times of 10:30 a.m., 10:00 a.m., and 09:30 a.m., respectively. GOME provides global data from 1996 to June 2003 having a spatial resolution of $40 \times 320\,\mathrm{km^2}$. In addition, data from January 2003 to February 2008 for SCIAMACHY having a spatial resolution of $30 \times 60\,\mathrm{km^2}$ and from March 2007 to February 2008 for GOME-2 ($40 \times 80\,\mathrm{km^2}$) have been used here. Monthly mean values were calculated on a grid of $0.125^\circ \times 0.125^\circ$. Table 1 describes some relevant instrumental parameters.

The retrieval approach used to determine NO_2 columns from the nadir measurements by the satellite instruments is based on the Differential Optical Absorption Spectroscopy (DOAS) method. This technique determines the NO_2 slant column density, SCD, along the light path through the atmosphere in the spectral window between 425 and 450 nm by separating high frequency molecular signatures from broadband absorption and scattering (Brewer et al., 1973; Noxon, 1975; Platt et al., 1979). In order to retrieve tropospheric amounts of NO_2 the technique known as tropospheric excess method (TEM) has been employed. This relies on the longitudinal homogeneity of the stratospheric column at the same local time. Comparison of the measurements at a given location with the mean SCD in a reference region of the same latitude, here chosen to be from 180° E to 140° W, yields the tropospheric excess SCD. This approach assumes implicitly that the tropospheric amount of NO_2 in this reference region

Table 1. Some relevant parameters of the satellite data used and the model.

	Covered Period	Local Time	Resolution (km^2)
GOME	1996–2002	10:30	40×320
SCIAMACHY	2003–2008	10:00	30×60
OMI	2004–2008	13:45	24×13
GOME-2	2007–2008	09:30	40×80
E5/M1	2000–2005[a] (2001)[b]	09:30–10:30	2.8°×2.8°

[a]Period of used ECMWF data.

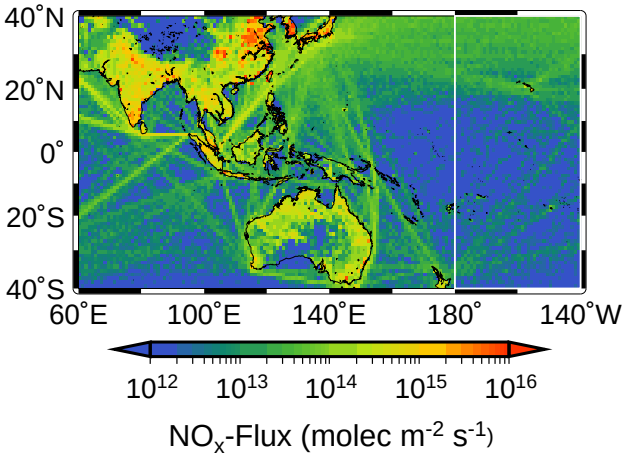

Fig. 1. NO_x emissions inventory as used in the model simulation. Estimates are taken from EDGAR3.2FT2000 over land and from Eyring et al. (2005) for ship emissions. The reference sector used in the tropospheric excess method (TEM) from 180° to 140° W is marked by the white box.

is negligible (Fig. 1). The SCD can be converted to a vertical column density (VCD) by division with an Air Mass Factor (AMF). The AMF corrects for the different sensitivity of measurements to absorption in different altitudes, which is determined by the relative penetration depth and depends on the magnitude of the surface spectral reflectance and multiple scattering within the atmosphere. This is of particular importance for absorbers located close to the surface. The resulting tropospheric excess column is denoted as TEC. This method belongs to a family of retrieval approaches called residual techniques. The analysis used here is described in Richter et al. (2004). The main assumptions made for the airmass factors are a surface albedo of 4%, a well mixed boundary layer of 700 m and a cloud threshold of 20%. More detailed descriptions of the retrieval method can be found in Richter and Burrows (2002) and in Burrows et al. (1999). Uncertainty is introduced into the satellite columns in the different steps of the analysis: the fitting of the slant columns, the correction of the stratospheric contribution, the assumptions made for the airmass factor and contamination by residual clouds. An additional source of variability is the sparse coverage in particular of SCIAMACHY measurements which can lead to sampling artifacts as only few measurements contribute to the monthly average. A detailed discussion of the error budget of satellite measurements is given in Boersma et al. (2004). However, for this specific application, the relative importance of the different error contributions differs from that presented for the global data set.

In Table 2, an overview is given on the random errors estimated from the slant columns retrieved over a clean region, the number of measurements per month in the region S analysed (see Sect. 3.1 for the definition) and the resulting random error. While the values differ between the instruments as a result of pixel size and measurement pattern, the overall result is similar with a monthly random error of about 4×10^{13} molec cm^{-2}. This value is small in comparison to the estimated AMF errors which are of the order of 30% (or about 2×10^{14} molec cm^{-2}), mainly from the uncertainty of aerosol effects as discussed below.

In other studies, the vertical profile of NO_2 used in the airmass factor calculations has been taken from the model calculations to assure consistency between model and measurement. However, in the case of shipping emissions, the coarse resolution model cannot provide a good representation of the vertical NO_2 distribution in the small region affected by shipping emissions, and using the model profile would lead to airmass factors not apporpriate for the retrieval of shipping NO_2. Consequently, we here have used a simple box model of the NO_2 distribution assuming a well mixed boundary layer of 700 m height and no NO_2 in the rest of the troposphere. Analysis of the vertical sensitivity of the measurements shows that this is not a critical assumption – changing the mixing height to 300 m or 1000 m respectively changes the airmass factor by only about ±10%. The same airmass factor has been used for both the shipping region and for the control regions. This is argued to be acceptable for the present study for the following reason. If we assume that the NO_2 which is not resulting from ship emissions is the same over the shipping region as in the control areas, the same error will be made in both regions and therefore cancel in the difference. Therefore, differences between the regions can be attributed to real column differences. However, the absolute NO_2 amount in the reference regions B1 and B2 will be overestimated by this approach by up to 40% compared to an analysis using for example an *a priori* with the NO_2 distributed evenly between the surface and 5 km. While this is a significant uncertainty, it is not critical as the data from the reference regions will not be used for the quantitative interpretation of the shipping signal.

Aerosols can have a significant impact on the radiative transfer in the atmosphere. For satellite nadir observations

Table 2. Overview on estimates of random and systematic uncertainties in the satellite data. Random errors are estimated from data for one year for average sampling; the spread of values between months is given in brackets.

Instrument	GOME (1997)	SCIAMACHY (2006)	GOME-2 (2007/2008)
Uncertainty of individual fits	5×10^{14} molec cm^{-2}	1×10^{15} molec cm^{-2}	1.2×10^{15} molec cm^{-2}
Average number of values per month in region S (range given in brackets)	165 (90–260)	650 (300–1000)	1250 (800–1500)
Random uncertainty of monthly average over region S	4×10^{13} molec cm^{-2}	4×10^{13} molec cm^{-2}	3.5×10^{13} molec cm^{-2}
Uncertainty of AMF		30%	
Uncertainty from clouds		<10%	
Uncertainty of cross-sections		5%	

of tropospheric absorption, both enhancement and reduction of sensitivity can result from aerosols, depending on their vertical distribution relative to the NO_2 and their single scattering albedo (SSA). Sensitivity studies assuming different amounts of aerosols with different SSA have shown, that for an aerosol that is mixed within the NO_2 layer, the net effect is surprisingly small (of the order of 5% for AOD 0.1 and of the order of 30% for AOD of 0.5 for a well mixed layer of 700 m) unless the aerosol is highly absorbing. This is the largest contribution to the uncertainty of the airmass factor.

Additional uncertainties are related to residual clouds present in the measurements in spite of the cloud fraction threshold applied. Any NO_2 below clouds will be underestimated while low clouds or dense aerosol will tend to enhance the visibility of the NO_2 above them. To investigate the possible impact of clouds, the GOME-2 data set was analysed using different cloud fraction thresholds from 5% to 100%. For most of the months, the results agreed within 10% for cloud fraction thresholds between 10% and 30%, indicating largely compensating effects of clouds. No clear evidence could be found for increasing NO_2 columns at cloud thresholds smaller than 20% but NO_2 signals systematically decreased for cloud fractions of 50% or larger. We therefore estimate the cloud related uncertainty for the shipping NO_2 to be smaller than 10%. In particular for SCIAMACHY, the irregular sampling pattern can also introduce uncertainties which in individual months can become significant. This is a result of the small spatial extent of the shipping signal in combination with the limited coverage of SCIAMACHY measurements. The effect can in principle be reduced by sampling the model only at the time and location of an actual measurement (van Noije et al., 2006) but this was not possible in this study as high spatial resolution would be needed in the model data to properly simulate the effect.

The overall accuracy of the retrieved columns over the region of interest (S) can be summarised to be 40%+4 $\times10^{13}$ molec cm^{-2} for a monthly average.

2.2 Model description

ECHAM5/MESSy1 (hereafter referenced as E5/M1) is an Atmospheric Chemistry General Circulation Model (ACGCM) (Jöckel et al., 2006). The applied spectral resolution is T42, corresponding to a quadratic-gaussian grid of approximately 2.8°×2.8° in longitude and latitude, respectively. The used model setup has 90 layers on a hybrid-pressure grid reaching up to 0.01 hPa. Details of the E5/M1 simulation S1 that is used in this study are described in Jöckel et al. (2006). In order to be able to directly compare the model results with observations, the model dynamics has been nudged using operational analysis data from the European Centre for Medium-Range Weather Forecasts (ECMWF) from January 2000 to October 2005. The model integration time-step is 900 s. Output has been archived as 5-hourly instantaneous fields. This yields an hourly resolved diurnal cycle within 5 days of integration.

Anthropogenic and natural emissions of NO, CO, SO_2, NH_3 and several hydrocarbon species are taken from the EDGAR3.2FT2000 http://www.mnp.nl/edgar/model/v32ft2000edgar/docv32ft2000 dataset (Olivier et al., 2005). NO_x emissions include anthropogenic sources with an annual emission rate of 31 Tg(N) and biomass burning emissions with an annual emission rate of 9.3 Tg(N) (see electronic supplement to Pozzer et al., 2007) http://www.atmos-chem-phys.net/7/2527/2007/acp-7-2527-2007-supplement.pdf. Global NO_x emissions from lightning are 2 Tg(N) yr^{-1}. For comparison with satellite data the relevant E5/M1 parameters are given in Table 1. The E5/M1 model has been evaluated by comparison to the compiled tropospheric in-situ observations of Emmons et al. (2000) http://gctm.acd.ucar.edu/data/ and other observational data. These show that the model simulates tropospheric distributions of NO, HNO_3 and PAN concentrations over the tropical Ocean reasonably well (Jöckel et al., 2006).

Total anthropogenic NO_x emissions from shipping in the E5/M1 simulation are 6.3 Tg(N) yr^{-1} (Eyring et al., 2005)

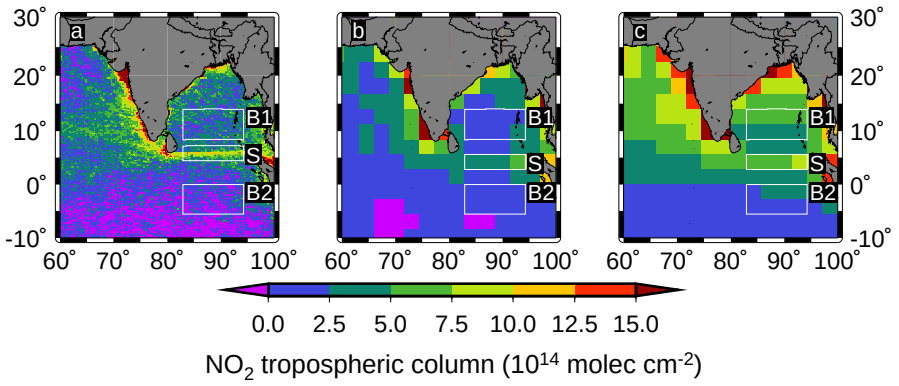

Fig. 2. February mean tropospheric NO_2 columns: **(a)** derived from SCIAMACHY measurements from 2003 to 2008 using the DOAS technique and the tropospheric excess method (TEM). **(b)** taken from the E5/M1 model using the TEM. **(c)** taken from the E5/M1 model integrating the NO_2 concentration up to approximately 200 hPa (SUM). The white boxes indicate the averaging regions used for further comparison.

and are distributed over the globe using AMVER as a spatial proxy. Since a parameterisation for sub-grid scale ship plume processes in global models is not yet available, the emission totals are instantaneously spread onto the large model grid box without accounting for sub-grid scale plume processes that cause dispersion, transformation and loss processes. The neglect of ship plume processes could cause an overestimation of the ship induced NO_x and ozone concentrations simulated by the model (see Eyring et al., 2009).

As a result of the model output being provided at full hours in universal time for every grid box and the ENVISAT satellite having a local equator crossing time of 10:00 a.m., the model data between 09:30 a.m. and 10:30 a.m. local time have been averaged in the regions of the ship emissions and the respective reference sectors. Furthermore, to reduce the effects of the inter-annual variability, a 6 year climatological average (2000–2005) of the model data has been used. A study of inter-annual changes is not performed as only the meteorological parameters are driven with inter-annual variability while the emission rates of pollutants, in particular from the highly variable biomass burning sources are constant for all years. Two techniques are applied to derive the tropospheric NO_2 columns from the model output. The first technique is consistent with the TEM employed for satellite data. The total columns are derived by vertically integrating over all layers of the atmosphere. NO_2 TECs are then calculated by subtracting the mean total column at the same latitude in a reference sector over the Pacific from the total column at a given location. These NO_2 columns are hereafter denoted as E5/M1(TEM). In the second approach, the column is calculated by integrating the NO_2 amount over the lowest 20 model layers (approx. up to 200 hPa), in the following denoted as E5/M1(SUM).

In addition, the results of a second E5/M1 simulation performed in the scope of the EU-project QUANTIFY are used (Hoor et al., 2009). In this simulation, all model parameters are identical to the evaluation simulation described above, with the exception of the following: Global NO_x emissions from international shipping are specified at 4.4 Tg(N) yr^{-1} as estimated by Endresen et al. (2007), lightning NO_x emissions are set to 5 Tg(N) yr^{-1}. There are also differences in the emissions from road traffic and aviation, but these do not affect the region discussed in this study. NO_2 TECs from this simulation are denoted as E5/M1(QFY).

3 Results and discussion

3.1 Comparison of model and SCIAMACHY data

The shipping lane from the southern tip of the Indian subcontinent to Indonesia in the north eastern Indian Ocean has been selected to verify ship induced NO_x, because here ship traffic is concentrated in a narrow line and other local NO_x emissions are negligible. For a quantitative comparison of the model results and the satellite data three regions (S, B1, and B2) depicted in Fig. 2 are defined. The region S is the box which contains the shipping lane. The region B1 is north of the shipping lane and the region B2 is south of the lane. Both B1 and B2 are assumed not to be significantly influenced by emissions from shipping. All regions have a longitudinal width of four model grid boxes from 83° E to 94.2° E. The regions B1 and B2 have a latitudinal width of two model boxes: B1 extending from 8.4° N to 14° N and B2 from 5.6° S to the equator. The position of the modelled shipping lane (Fig. 2b) is shifted relative to the observed shipping lane (see below). Therefore the region S is defined as the grid box extending from 2.8° N to 5.6° N. For the satellite data, the region S has a latitudinal width of 2.8° centred around the maximum of the NO_2 enhancement in the given month, as shown by the white line in Fig. 3. NO_x ship emissions in region S are calculated from the global emission

Table 3. NO_x ship emissions from previous studies. The table summarizes the global emission total and the emission into region S (83° E–94.2° E/4.4° N–7.2° N) for different spatial ship activity patterns (AMVER and ICOADS). Emission rates for 2000 are scaled with the increase of total seaborne trade to the year 2005.

	2000 NO_x emissions in Tg(N) yr^{-1}			2005 NO_x emissions in Tg(N) yr^{-1}		
	Global	S (AMVER)	S (ICOADS)	Global	S (AMVER)	S (ICOADS)
Endresen et al. (2003)	3.63	0.052	0.041	4.45	0.063	0.050
Endresen et al. (2007)	4.4	0.063	0.050	5.39	0.076	0.061
Corbett and Koehler (2003)	5.93	0.084	0.067	7.28	0.103	0.082
Eyring et al. (2005)	6.36	0.090	0.072	7.81	0.111	0.088
Eyring et al. (2009)	5.18	0.074	0.059	6.36	0.090	0.072

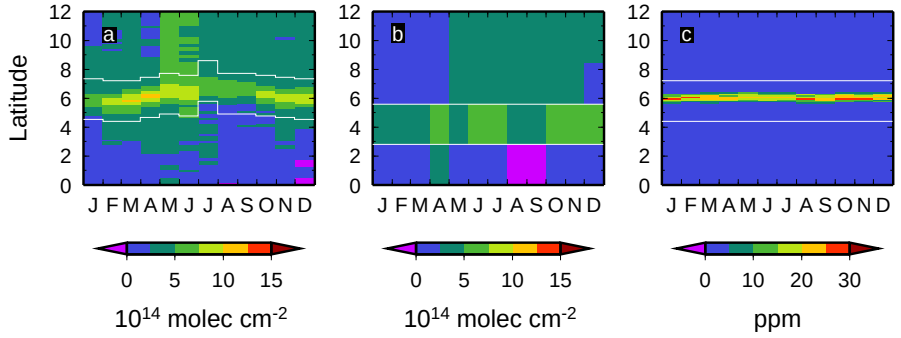

Fig. 3. Monthly zonal mean NO_2 tropospheric excess columns **(a)** derived from SCIAMACHY measurements from 2003 to 2008 using the DOAS technique and the tropospheric excess method (TEM); **(b)** derived from ECHAM5/MESSy1 model simulations from 2000 to 2005 and the TEM. **(c)** Zonal mean AMVER ship activity measured in ppm of global ship traffic (Wang et al., 2008). The zonal average includes data from 83° E to 94.2° E. White lines indicate the northern and southern border of region S.

totals of Endresen et al. (2003, 2007), Corbett and Koehler (2003) and Eyring et al. (2005, 2009) using ship activity patterns from AMVER and ICOADS, see Table 3. For the same global emission totals, the emissions that are assigned in the region of interest vary between AMVER and ICOADS because of the difference in the spatial proxy. In region S the emissions range from 41 Gg(N) yr^{-1} (Endresen et al., 2003 with ICOADS) to 90 Gg(N) yr^{-1} (Eyring et al., 2005 with AMVER), i.e. depending on the inventory the emission estimates differ by more than a factor of 2.

In Fig. 2, the mean February NO_2 tropospheric column amount, derived from all available SCIAMACHY measurements between 2003 and 2008 is compared to E5/M1 (TEM) and E5/M1 (SUM). The shipping lane in the satellite data is identified by the region having NO_2 TEC of about 10×10^{14} molec cm^{-2} in comparison to the surrounding region, where values of around 2×10^{14} molec cm^{-2} are found. The width of the shipping lane is approximately 1° in latitude or 110 km (Fig. 2a).

While the overall agreement with E5/M1 (TEM) data is good, the coarse horizontal resolution of the model becomes apparent (Fig. 2b). The shipping signature in the model data is shifted southward relative to the satellite measurements. This is the result of two regridding steps: First from the $0.1°\times0.1°$ grid of the ship activity pattern to the $1°\times1°$ grid of the emission data base, and subsequently to the $2.8°\times2.8°$ resolution of the model. Qualitatively, as the model grid box is approximately twice as large as the width of the measured shipping lane the maximum is expected to be reduced from 10×10^{14} molec cm^{-2} to 5×10^{14} molec cm^{-2}.

The difference between E5/M1 (TEM) and E5/M1 (SUM) is about 2.5×10^{14} molec cm^{-2}, with the satellite data being in better agreement with the E5/M1 (TEM) data. While Fig. 2 only shows February, this is valid for all months. This underlines the importance of choosing a consistent data analysis method for the comparison of model and satellite data. In the following analysis only E5/M1 (TEM) is used.

Figure 3 compares zonal mean (83° E to 94.2° E) NO_2 TEC derived from SCIAMACHY to E5/M1 (TEM) and the AMVER ship activity pattern as a function of time and latitude. The shipping lane is discernible by enhanced values of NO_2 TEC throughout the year in the satellite data (Fig. 3a). However, the latitudinal position of the maximum enhancement varies over the year, being further south in the northern hemispheric winter months and further north in the summer. Additionally, the width of the shipping lane and the

magnitude of TEC changes over the year. In January and from July to September the signature of ship emissions on the NO_2 TECs spreads over a larger area and the maximum is less pronounced, never rising above 7.5×10^{14} molec cm^{-2}. In the E5/M1 model data this seasonal pattern cannot be resolved as a result of the coarse model resolution (Fig. 3b). As the ship traffic from AMVER data (Wang et al., 2008) in this region shows no distinct seasonality (Fig. 3c; from AMVER data, Wang et al., 2008), this seasonal variation is attributed to the changing meridional wind patterns over this region. In the summer the wind comes mainly from the south whereas in winter it comes from the north. This seasonal variation was also observed by Beirle et al. (2004) in GOME data. The correlation of the latitude of the maximal NO_2 TEC with the mean meridional wind derived from ECMWF reanalysis data is 0.75, i.e. a reasonably strong correlation. In addition, in the satellite data of NO_2 TEC, a significant seasonality over the Bay of Bengal north of the shipping lane between 8° N and 12° N is observed in the months May and June. The possible reasons for this behaviour are discussed below.

3.2 Analysis of NO_2 TEC from the different instruments and the model

Figure 4 shows the mean NO_2 tropospheric excess column for three different instruments compared to the model output in the selected regions S, B1, and B2. For each month the mean of all available years has been calculated from GOME (8 years), SCIAMACHY (5 years), GOME-2 (1 year), and E5/M1 data (6 years). The standard deviation of the averaged data comprises instrument noise plus atmospheric variability of NO_2 and is depicted as errorbars in Fig. 4. As the local time of model data in the regions is centred around 10:00 LT the most direct comparison is between SCIAMACHY and E5/M1(TEM), reducing potential differences through diurnal variations in NO_x. In general SCIAMACHY and E5/M1 (TEM) are in good agreement, having a RMS-difference of 0.8×10^{14} molec cm^{-2}. In region B1 SCIAMACHY is somewhat higher than E5/M1 (TEM) in March and May, while in region B2 SCIAMACHY is somewhat higher than E5/M1 (TEM) in September and October. The small discrepancies in region B1 and B2 coincide with the biomass burning seasons in adjacent landmasses as seen in the TRMM Fire Index http://tsdis.gsfc.nasa.gov/tsdis/Fire/monthly_archive.html, i.e. typically February to May/June in India and the Indochinese Peninsula and from August to October in Indonesia. As the EDGAR3.2FT2000 dataset is valid for the year 2000 and SCIAMACHY measurements are from 2003 to 2008 discrepancies between model input and actual biomass burning emissions can be expected.

The GOME and GOME-2 measurements are consistent with SCIAMACHY data within errorbars in the regions S, B1, and B2 throughout the year. One exception is the large value of GOME-2 in January 2008. As the NO_2 TEC measured by SCIAMACHY in January 2008 is also enhanced in

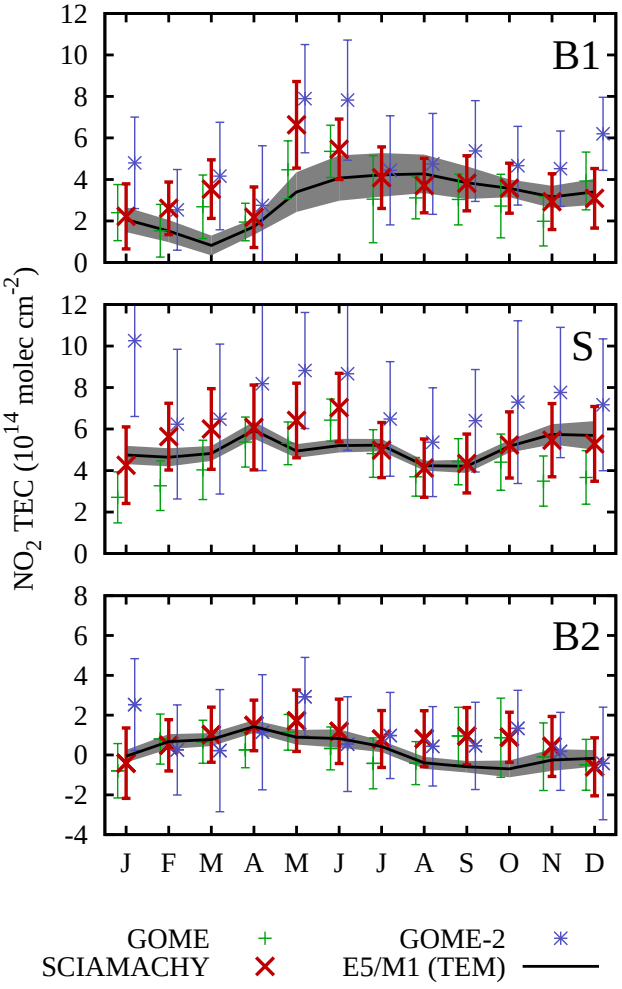

Fig. 4. Monthly mean NO_2 tropospheric column in three selected regions over the Indian Ocean. Satellite data from SCIAMACHY, GOME and GOME-2 are denoted by symbols. For model output columns are derived by tropospheric excess method (TEM). The shaded area for the model simulations shows the interannual standard deviation.

comparison to former years (not shown), we consider this to be a result of a unique situation occurring in this month. As this deviation happens in all three regions, it is considered not to be related to the ship traffic and is not further discussed in this study. The observation of enhanced NO_2 TEC by all three instruments compared to model results in region B1 in March and May and in region B2 in September and October indicates that they do not result from a bias inherent to SCIAMACHY, but reflect variations in tropospheric NO_2 content.

While monthly means among the satellite instruments are consistent within errorbars, the annual mean NO_2 TEC over the regions S differ among the instruments (Fig. 5). Possible explanations of this difference in TEC NO_2 over region S are

(i) changes of ship emissions over time,

(ii) diurnal variation of NO_2,

(iii) change of background NO_x field,

(iv) instrumental bias.

In the following we will discuss these aspects in more detail.

(i) Over the last 30 years a clear and well understood correspondence is observed between fuel consumption and seaborne trade in tonne miles [1], because the energy required in global trade is proportional to the physical work performed (Eyring et al., 2009). The total seaborne trade volume (STV) has risen from 20 968 tmi in 1996 to 31 847 tmi in 2007 (Fearnleys, 2007). As no significant measures of NO_x-reductions have been introduced, we use the increase in STV over this period as an indicator for NO_x emissions increase. The rise in STV over the time period covered by GOME measurements (1996–2002) is 15% with a mean STV of 22 549 tmi, while it is a 21% increase with a mean value of 29 021 tmi over the time period of SCIAMACHY observations (2003–2008). The mean STV for the SCIAMACHY measurement time period is 29% higher than the mean STV for GOME observations, while it is 10% lower than the mean STV of 31 847 tmi during the time period of GOME-2 measurements (2007–2008).

In order to assess the difference in the measurements that is due to the raise in NO_x emissions, linear regression on the monthly mean NO_2 TECs (this time without inter-annual average) was performed. Linear regression over 84 months of GOME measurements in region S yields a slope of $(0.0\pm0.13)\times10^{14}$ molec cm^{-2} yr^{-1}, which corresponds to (0±22)% of the mean NO_2 TEC of all available GOME data. For the 67 month of SCIAMACHY measurements the regression gives a slope of $(0.15\pm0.15)\times10^{14}$ molec cm^{-2} yr^{-1} (14±14%). This implies that no significant trend is discernible within the uncertainties over the periods of measurements of either GOME or SCIAMACHY. However, the change in mean NO_2 TEC between the measurement periods of GOME and SCIAMACHY has increased by (26±15)%, which is in agreement with the rise of 29% in STV (Fig. 5). On the other hand, the mean NO_2 TEC as observed by GOME-2 from 2007 to 2008 is (37±22)% higher than the mean NO_2 TEC over the period of measurement of SCIAMACHY (2003–2008), which is substantially higher than what would be expected from the 10% rise of the mean STV.

(ii) The diurnal variation of NO_2 mainly arises from variation of its photodissociation rate and the effective first order removal rate for its reaction with OH. As a result of these two processes NO_2 decreases during the morning. Additionally a diurnal variability could result from a diurnal variation of the emissions as has recently been observed in satellite data (Boersma et al., 2008), but this is not to be expected in the case of shipping. As the equator crossing times of GOME-2, SCIAMACHY and GOME are 09:30, 10:00, and 10:30 LT, respectively, the instruments see different parts of this diurnal cycle. To investigate whether the observed differences can be explained by the diurnal cycle, the mean NO_2 TECs from GOME and SCIAMACHY are compared for the period August 2002 to June 2003 and for the period March 2007 to February 2008 for SCIAMACHY and GOME-2. By confining the analysis on these time periods the seasonal and inter-annual variation is removed from the data. In addition, the diurnal variation between 09:30 a.m. and 10:00 a.m. and between 10:00 a.m. and 10:30 a.m. in mean NO_2 TEC in region S is calculated from all E5/M1 (TEM) results.

Over the region S the model predicts a decrease in mean NO_2 TEC of $0.6–0.7\times10^{14}$ molec cm^{-2} over the half of an hour between the respective equator crossing times (Fig. 6). However, the difference in mean NO_2 TEC derived from GOME and SCIAMACHY measurements from 2002/2003 show no significant decrease over this half hour (green data in Fig. 6). On the other hand, the difference in mean NO_2 TEC measured by GOME-2 and SCIAMACHY in 2007/2008 is about $(1.6\pm1.4)\times10^{14}$ molec cm^{-2} in region S, and therefore greater than predicted by the model (blue data in Fig. 6).

In addition to the three instruments GOME, SCIAMACHY, and GOME-2, the instrument OMI measures NO_2 at a local time of 13:45. Therefore, diurnal variations should become particularly clear in the difference between OMI

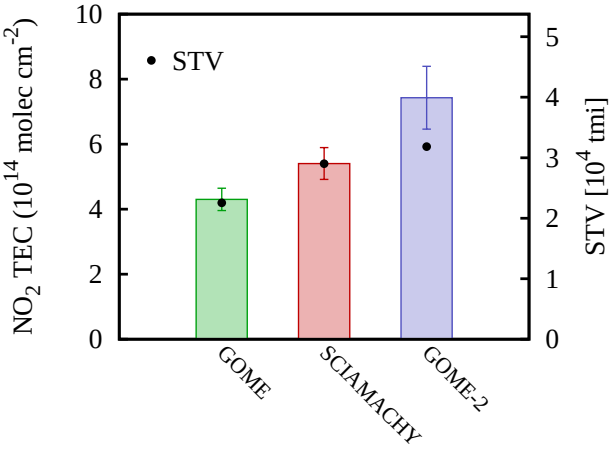

Fig. 5. Multiannual mean NO_2 tropospheric excess column (TEC) measured with satellite instruments GOME (1996–2003), SCIAMACHY (2002–2008), and GOME-2 (2007–2008) over region S over the Indian Ocean. Errorbars are based on the estimate of the uncertainties excluding the AMF contribution which is assumed to be the same for all three data sets. In addition, the mean seaborne trade volume (STV) over the corresponding time periods is given (•).

[1]The unit *tonne mile* or tmi as a measurement of trade volume is defined as the product of the distance that freight is transported, measured in miles, and the weight of the cargo being shipped, measured in tons.

and SCIAMACHY. Here, we use operational OMI total NO_2 slant columns as provided by NASA (Buscela et al., 2006) to investigate the possible diurnal effect. While the stratospheric correction and airmass factors are applied as for the other products, the slant column fit as well as the cloud retrieval algorithm used for OMI differs from that applied for the other instruments. Therefore, this data set can not be considered as being fully consistent with the other time-series.

The yellow data in Fig. 6 show that the difference between the columns from these two instruments is smaller than expected from model calculations. However, as discussed before, the OMI NO_2 slant columns are not retrieved in a way fully consistent with that used for the other three instruments, and therefore these results could be impacted by retrieval biases.

(iii) Another explanation for the differences observed could be a change in background NO_x levels due to a change of outflow of NO_x from adjacent landmasses (Kunhikrishnan and Lawrence, 2004). A detailed assessment of such possible changes requires additional data on changes in continental sources which are not readily available. As this is not related to the main topic of this paper which focuses on ship induced NO_2 over the Indian Ocean it is not further pursued.

(iv) Finally it should be mentioned that instrumental bias can cause some of the differences between the data sets. Such a bias could either be relative, e.g. from uncertainties in cross-sections but also absolute, e.g. from calibration issues. Relative differences should have a similar pattern for all three regions studied, and as can be seen in Fig. 4, this does not appear to be the case as the difference between data from the various instruments can not be explained by a simple factor. Absolute biases could explain part of the higher GOME-2 columns in regions B1 and S, but as the reference sector method is used, most additive effects should cancel in the TEC. We therefore conclude that instrumental effects alone can not explain the observations.

In conclusion, the data from the satellite instruments, which measure at different local times, yield different mean NO_2 TECs over the region S. These differences between the retrieved columns of NO_2, attributed to emissions from shipping, exhibit a behaviour similar to that expected from the diurnal variation of NO_2 and the increase in NO_x emission from the growing STV. However, the magnitudes of the modelled and the observed differences are not identical. This in part is explained by slight differences in the retrieval procedures and in model uncertainties. Taking the uncertainties on the NO_2 columns retrieved from the satellite measurements and the modelled diurnal variation into account, the results are consistent with an increase in shipping emissions over the shipping lanes in the Indian Ocean, but the uncertainty, comprising both retrieval and model error and variability in the atmosphere, are such that no firm conclusion can be drawn as to the magnitude of the observed changes.

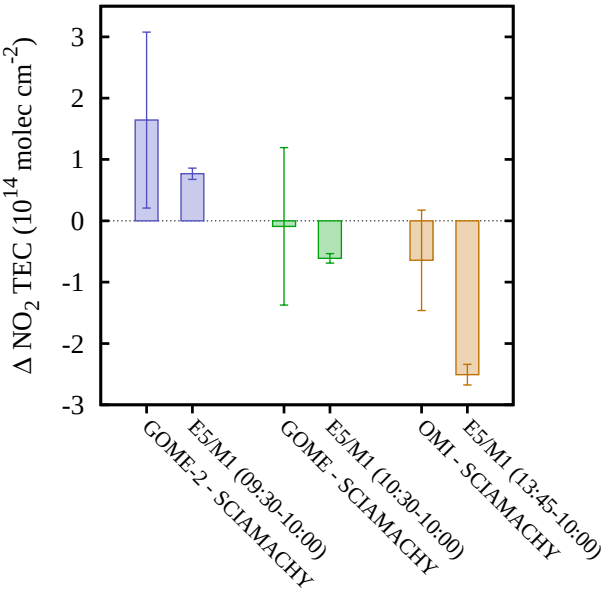

Fig. 6. Difference in mean NO_2 TEC (Δ NO_2 TEC) as a result of diurnal variation in tropospheric NO_2 over the region S estimated from satellite measurements compared to the corresponding Δ NO_2 TEC from model simulations. The differences in NO_2 TEC between GOME-2 (09:30 a.m.) and SCIAMACHY (10:00 a.m.) measurements are calculated for the period from March 2007 to February 2008, the differences in NO_2 TEC between GOME (10:30 a.m.) and SCIAMACHY (10:00 a.m.) measurements are calculated for the period from August 2002 to June 2003 and the differences in NO_2 TEC between OMI (13:45 a.m.) and SCIAMACHY (10:00 a.m.) measurements are calculated for the period from October 2004 to February 2008. The error bar for the model simulations shows the interannual standard deviation.

3.3 Evaluation of ship emission inventories

As the NO_2 level over the ship influenced region S comprises ship induced and background NO_x, the results of the model calculation E5/M1 (QFY) are evaluated in addition in the regions B1, S, and B2 to estimate the sensitivity of the NO_2 TEC to NO_x ship emissions. The main differences between E5/M1 (TEM) and E5/M1 (QFY) are the amount of traffic induced NO_x emissions and the amount of lightning NO_x. The annual average NO_2 TEC of the year 2003 over the regions B1 and B2 which are not affected by ship emissions show only minor differences between E5/M1 (TEM) and E5/M1 (QFY) (Fig. 7). On the other hand, the two model simulations differ over the ship influenced region S with E5/M1 (TEM) being 2×10^{14} molec cm^{-2} higher than E5/M1 (QFY). The ship induced NO_x emission strength is the only relevant difference between the two model simulations in region S. We therefore conclude that the NO_2 TEC over region S is mainly controlled by ship induced NO_x and other sources such as lightning play only a minor role.

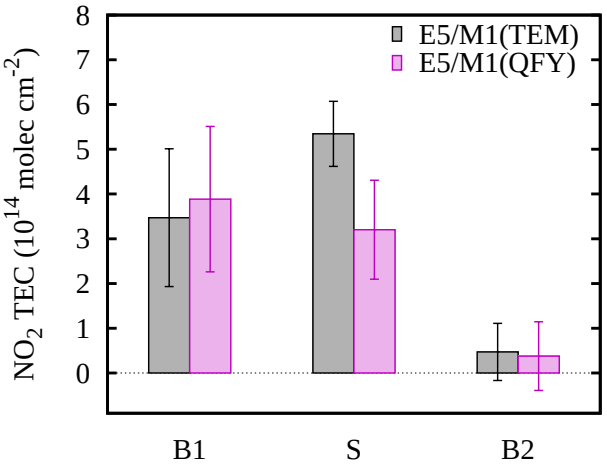

Fig. 7. Mean NO_2 TEC for the year 2003 over the three regions studied from E5/M1(TEM) and E5/M1(QFY). The main difference between the two model runs is the shipping emissions inventory used. The error bar for the model simulations shows the interannual standard deviation.

To evaluate the ship emission inventories used in the model simulations, the NO_2 TEC over the region S from E5/M1 (TEM) and E5/M1 (QFY) are correlated to the measured NO_2 TEC from GOME and SCIAMACHY (Fig. 8). As stated in the previous paragraph E5/M1 (QFY) values are lower than those of E5/M1 (TEM). In comparison to GOME measurements NO_2 TEC from E5/M1 (TEM) tend to be higher than those measured and E5/M1 (QFY) values tend to be lower (Fig. 8a). The RMS deviation between NO_2 TEC by GOME and E5/M1 (TEM) is 1.3×10^{14} molec cm^{-2} and 1.8×10^{14} molec cm^{-2} between GOME and E5/M1 (QFY). Therefore GOME NO_2 TECs are in slightly better agreement with E5/M1 (TEM), indicating an emission rate somewhere below 6.3 Tg(N) yr^{-1} over the period of GOME measurements (1996–2003). On the other hand, SCIAMACHY NO_2 TECs are in much better agreement with E5/M1 (TEM) than with E5/M1 (QFY), the RMS deviation being 0.8×10^{14} molec cm^{-2} and 2.5×10^{14} molec cm^{-2}, respectively. This indicates that the global emissions of 6.3 Tg(N) yr^{-1} used in the E5/M1 (TEM) model run are much more consistent with the satellite data of NO_2 TEC over region S in the period 2002–2008 than the lower value of 4.4 Tg(N) yr^{-1} used in E5/M1 (QFY).

3.4 Error analysis

Uncertainties of the data shown as errorbars in the figures are derived by statistical analysis of the averaged values. This includes both instrumental error and actual variation in tropospheric NO_2 content. The model E5/M1 shows in general less variation than the satellite data (Fig. 4) as the model uses the same emission scenario for all years, whereas actual emissions show a variation over the years.

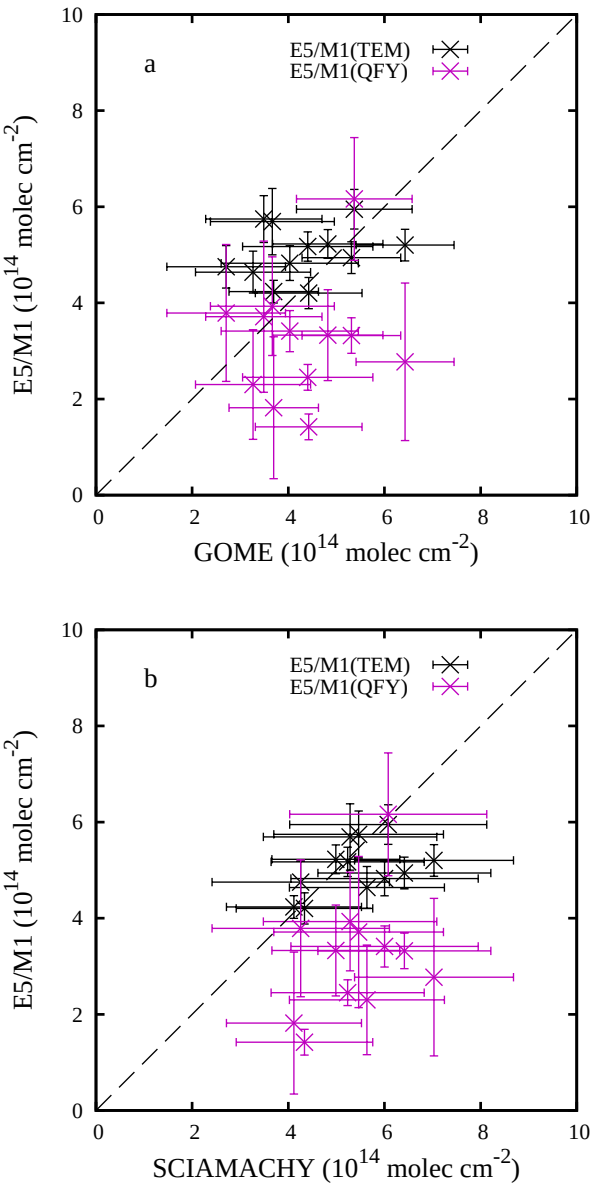

Fig. 8. NO_2 tropospheric column over the shipping lane from India to Indonesia (S). Monthly satellite values, averaged over all available years from **(a)** GOME and **(b)** SCIAMACHY are correlated to the model results E5/M1(TEM) and E5/M1(QFY). The error bar for the model simulations shows the interannual standard deviation.

Systematic errors are more difficult to quantify. Those systematic errors, which apply similarly to the data in the Indian and the Pacific Ocean, cancel each other due to the use of the TEM. While this does apply to most of the errors, some differences between the reference region and the area studied here could still introduce systematic errors. One example is the effect of vibrational Raman scattering in ocean water which can interfere with the NO_2 satellite retrieval. However, there is no indication in the data that such effects lead to

significant problems in this study. Comparison of local measurements with model calculation indicate an overestimation of modelled NO_2 (Kasibhatla et al., 2000; Davis et al., 2001). Our results on the other hand do not indicate such an overestimation. Furthermore, we are of the opinion that our comparison of large scale measurements with large scale models, which takes the used retrival method (TEM) into account, is more consistent than the comparison of local measurements with large scale calculations.

One source for systematic error in the model calculations which does not cancel out is neglecting small scale plume processes. While several studies have addressed this issue, none of the plume model studies has provided a sophisticated plume parameterisation or a simple reduction factor for the NO_x emissions that could be applied to global models. The step from case studies to a suitable parameterisation of subgrid-scale processes in global models has yet to be made for both gaseous and particulate emissions. However, several box model studies on ship plumes showed that the lifetime for NO_x is significantly shortened if plume chemistry is considered (e.g. Davis et al., 2001; Song et al., 2003; Charlton-Perez et al., 2009). The shortened NO_x lifetime could explain a significant fraction of the overprediction of NO_x levels in and near shipping lanes that was found in comparison of global chemistry models with observations (Lawrence and Crutzen, 1999; Davis et al., 2001). It can therefore be assumed that a consideration of sub-grid scale ship plume processes in global model simulation would reduce the simulated enhancement in NO_x concentration due to ship emissions providing additional support for the higher ship emission inventory.

4 Conclusions

Ship emissions of NO_x in the Indian Ocean have been analysed with the help of measurements from GOME (1996–2002), SCIAMACHY (2003–2007), and GOME-2 (2007/2008) in comparison to two global model simulations using different inventories. The Differential Optical Absorption Spectroscopy (DOAS) method and the tropospheric excess method (TEM) were used to retrieve NO_2 tropospheric excess columns (TECs) in the northern Indian Ocean. The satellite data was compared to NO_2 TEC retrieved from the output of a nudged simulation with the atmospheric chemistry general circulation model ECHAM5/MESSy1 (2000–2005). The shipping route from India to Indonesia can be detected in satellite data with an enhancement in NO_2 TEC of about 8×10^{14} molec cm^{-2}. The monthly variation of the latitudinal position of the NO_2 enhancement could be verified in the SCIAMACHY data. A correlation of 0.75 was found between the latitudinal position of the maximal NO_2 enhancement and the mean meridional wind speed derived from ECMWF reanalysis data.

For detailed analysis three regions were defined, one including the shipping lane (S), one in the Bay of Bengal (B1) and one over the free Indian Ocean (B2). B1 and B2 are assumed not to be influenced by ship emissions. Overall comparison of SCIAMACHY NO_2 TEC and E5/M1 TEC in the defined regions shows good agreement with SCIAMACHY being somewhat higher in B2 in August to November and somewhat higher in S and B1 in March and May. These differences in NO_2 TEC coincide with biomass burning seasons on landmasses nearby, i.e. February to May over India and the Indochinese Peninsula and August to October over Indonesia.

An analysis of differences between mean NO_2 TEC values in region S shows that GOME-2 has a $(2\pm1)\times10^{14}$ molec cm^{-2} higher TEC than SCIAMACHY. In comparison the NO_2 TEC as measured by GOME and SCIAMACHY differs by only $(1.1\pm0.6)\times10^{14}$ molec cm^{-2}. OMI data yield lower columns than those of SCIAMACHY by about 5×10^{14} molec cm^{-2}, but the retrieval used is not fully consistent with that of SCIAMACHY which could result in differences in the results. Two effects with possible contributions to these differences were analysed: First, the diurnal cycle of NO_2 as the four instruments measure NO_2 at slightly different times during the day (GOME-2 at 09:30 a.m.; SCIAMACHY at 10:00 a.m.; GOME at 10:30 a.m.; OMI at 01:45 p.m.), and second, the change in NO_x ship emissions over the measurement period. The diurnal variation observed has the same direction as predicted by the model but does not agree quantitatively even if data is limited to periods of overlapping measurements. As the temporal variability of the measurement data is large, no firm conclusion can be drawn using the limited dataset available.

Some of the difference can be attributed to the difference in the measurement period as ship emissions in the shipping lanes from 1996 to 2007 are expected to have increased as result of increase traffic. Linear regression has been used to study the trend in NO_2 TEC within the measurement period from either GOME or SCIAMACHY. From the trend analysis no statistically significant change in NO_2, i.e. larger than twice the standard deviation, was identified. However, the difference of (26 ± 15)% in mean NO_2 TEC between the measurements by GOME and SCIAMACHY is consistent with the rise of 29% in mean seaborne trade volume between the time periods of GOME and SCIAMACHY observations, indicating that emission have increased as expected.

Finally, the NO_2 TEC measurements were compared to the calculations of a second model run using a ship emission inventory of about 4 Tg(N) yr^{-1}. Here the differences between model and measurements are higher than in the first calculation, in particular for the SCIAMACHY time period. Therefore we conclude, that a ship emission inventory with around 6 Tg(N) yr^{-1} globally resulting in around 90 Gg(N) yr^{-1} in the region of interest when using the Automated-Mutual-Assistance Vessel Rescue System

(AMVER) as spatial proxy provides better agreement with measurement in the Indian Ocean than lower ship emissions estimates of 3–4 $Tg(N)\,yr^{-1}$ globally.

This study is based on data from a small region which is favorable for satellite retrievals of shipping emissions. A more extensive comparison of the ship emission inventories on the global scale is necessary to strengthen the results. Further studies are also needed on the effect of plume chemistry on the results of the coarse resolution model calculations to exclude a possible bias in the comparison to satellite derived columns.

Acknowledgements. This work has been supported by the Helmholtz-University Young Investigators Group SeaKLIM, which is funded by the Helmholtz Association of German Research Centres and the German Aerospace Centre (DLR). It has also been supported by the University and State of Bremen, the EU ACCENT network, and the EU-Project QUANTIFY. GOME and SCIAMACHY radiances and irradiances have been provided by ESA through DLR. GOME-2 radiances have been provided by EUMETSAT. OMI collection 3 NO_2 slant columns have been obtained from NASA. We would like to thank Ulrike Burkhardt and two anonymous reviewers for their helpful comments on the manuscript.

Edited by: O. Cooper

References

Buhaug, Ø., Corbett, J. J., Endresen, Ø., Eyring, V., Faber, J., Hanayama, S., Lee, D. S., Lee, D., Lindstad, H., Markowska, A. Z., Mjelde, A., Nelissen, D., Nilsen, J., Pålsson, C., Winebrake, J. J., Wu, W.-Q., and Yoshida, K.: Second IMO GHG study 2009, International Maritime Organization (IMO) London, UK, March 2009.

Beirle, S., Platt, U., von Glasow, R., Wenig, M., and Wagner, T.: Estimate of nitrogen oxide emissions from shipping by satellite remote sensing, Geophys. Res. Lett., 31, doi:10.1029/2004GL020312, 2004.

Boersma, K. F., Eskes, H. J., and Brinksma, E. J.: Error analysis for tropospheric NO_2 retrieval from space, J. Geophys. Res., 109, D04311, doi:10.1029/2003JD003962, 2004.

Boersma, K. F., Jacob, D. J., Eskes, H. J., Pinder, R. W., Wang, J., and van der A, R. J.: Intercomparison of SCIAMACHY and OMI tropospheric NO_2 columns: Observing the diurnal evolution of chemistry and emissions from space, J. Geophys. Res., 113, doi:10.1029/2007jd008816, 2008.

Bovensmann, H., Burrows, J., Buchwitz, M., Frerick, J., Noël, S., Rozanov, V., Chance, K., and Goede, A.: SCIAMACHY: Mission Objectives and Measurement Modes, J. Atmos. Sci., 56, 127–150, 1999.

Brewer, A., McElroy, C., and Kerr, J.: Nitrogen dioxide concentrations in the atmosphere, Nature, 246, 129–133, 1973.

Burrows, J., Hölzle, E., Goede, A., Visser, H., and Fricke, W.: SCIAMACHY – scanning imaging absorption spectrometer for atmospheric chartography, Acta Astronaut., 35, 445–451, 1995.

Burrows, J., Weber, M., Buchwitz, M., Rozanov, V., Ladstätter-Weißenmayer, A., Richter, A., DeBeek, R., Hoogen, R., Bramstedt, K., Eichmann, K., et al.: The Global Ozone Monitoring Experiment (GOME): Mission Concept and First Scientific Results, J. Atmos. Sci., 56, 151–175, 1999.

Bucsela, E. J., Celarier, E. A., Wenig, M. O., Gleason, J. F., Veefkind, J. P., Boersma, K. F., and Brinksma, E. J.: Algorithm for NO_2 vertical column retrieval from the ozone monitoring instrument, IEEE T. Geosci. Remote, 5, 1245–1258, 2006.

Callies, J., Corpaccioli, E., Eisinger, M., Hahne, A., and Lefebvre, A.: GOME-2- Metop's second-generation sensor for operational ozone monitoring, ESA Bull., 102, 28–36, 2000.

Charlton-Perez, C. L., Evans, M. J., Marsham, J. H., and Esler, J. G.: The impact of resolution on ship plume simulations with NO_x chemistry, Atmos. Chem. Phys. Discuss., 9, 8587–8618, 2009, http://www.atmos-chem-phys-discuss.net/9/8587/2009/.

Corbett, J., Fischbeck, P., and Pandis, S.: Global nitrogen and sulfur inventories for oceangoing ships, J. Geophys. Res., 104, 3457–3470, 1999.

Corbett, J. J. and Koehler, H. W.: Updated emissions from ocean shipping, J. Geophys. Res., 108, 4650, 2003.

Davis, D., Grodzinsky, G., Kasibhatla, P., Crawford, J., Chen, G., Liu, S., Bandy, A., Thornton, D., Guan, H., and Sandholm, S.: Impact of ship emissions on marine boundary layer NO_x and SO_2 distributions over the Pacific basin, Geophys. Res. Lett., 28, 235–238, 2001.

Emmons, L., Hauglustaine, D., Mueller, J., Carroll, M., Brasseur, G., Brunner, D., Staehelin, J., Thouret, V., and Marenco, A.: Data composites of airborne observations of tropospheric ozone and its precursors, J. Geophys. Res., 105, 20497–20538, 2000.

Endresen, Ø., Sørgård, E., Sundet, J., Dalsøren, S., Isaksen, I., Berglen, T., and Gravir, G.: Emission from international sea transportation and environmental impact, J. Geophys. Res., 108, 4560, 2003.

Endresen, Ø., Sørgård, E., Behrens, H. L., Brett, P. O., and Isaksen , I. S. A.: A historical reconstruction of ships' fuel consumption and emissions, J. Geophys. Res., 112, D12301, doi:10.1029/2006JD007630, 2007.

Eyring, V., Köhler, H. W., van Aardenne, J., and Lauer, A.: Emissions from international shipping: 1, The last 50 years, J. Geophys. Res., 110, D17305, doi:10.1029/2004JD005619, 2005.

Eyring, V., Stevenson, D. S., Lauer, A., Dentener, F. J., Butler, T., Collins, W. J., Ellingsen, K., Gauss, M., Hauglustaine, D. A., Isaksen, I. S. A., Lawrence, M. G., Richter, A., Rodriguez, J. M., Sanderson, M., Strahan, S. E., Sudo, K., Szopa, S., van Noije, T. P. C., and Wild, O.: Multi-model simulations of the impact of international shipping on Atmospheric Chemistry and Climate in 2000 and 2030, Atmos. Chem. Phys., 7, 757–780, 2007, http://www.atmos-chem-phys.net/7/757/2007/.

Eyring, V., Isaksen, I. S. A., Berntsen, T., Collins, W. J., Corbett, J. J., Endresen, Ø., Grainger, R. G., Moldanova, J., Schlager, H., and Stevenson, D. S.: Transport Impacts on Atmosphere and Climate: Shipping, Atmos. Environ., in press, doi:10.1016/j.atmosenv.2009.04.059, 2009.

Fearnleys: Fearnleys Review 2007, The Tanker and Bulk Markets and Fleets, Tech. rep., Fearnleys, 2007.

Hoor, P., Borken-Kleefeld, J., Caro, D., Dessens, O., Endresen, O., Gauss, M., Grewe, V., Hauglustaine, D., Isaksen, I. S. A., Jöckel, P., Lelieveld, J., Myhre, G., Meijer, E., Olivie, D., Prather, M., Schnadt Poberaj, C., Shine, K. P., Staehelin, J., Tang, Q., van Aardenne, J., van Velthoven, P., and Sausen, R.: The impact

of traffic emissions on atmospheric ozone and OH: results from QUANTIFY, Atmos. Chem. Phys., 9, 3113–3136, 2009, http://www.atmos-chem-phys.net/9/3113/2009/.

Jöckel, P., Tost, H., Pozzer, A., Brühl, C., Buchholz, J., Ganzeveld, L., Hoor, P., Kerkweg, A., Lawrence, M. G., Sander, R., Steil, B., Stiller, G., Tanarhte, M., Taraborrelli, D., van Aardenne, J., and Lelieveld, J.: The atmospheric chemistry general circulation model ECHAM5/MESSy1: consistent simulation of ozone from the surface to the mesosphere, Atmos. Chem. Phys., 6, 5067–5104, 2006, http://www.atmos-chem-phys.net/6/5067/2006/.

Kasibhatla, P., Levy, H., Moxim, W., Pandis, S., Corbett, J., Peterson, M., Honrath, R., Frost, G., Knapp, K., Parrish, D., and Ryerson, T.: Do emissions from ships have a significant impact on concentrations of nitrogen oxides in the marine boundary layer?, Geophys. Res. Lett., 27, 2229–2232, 2000.

Kunhikrishnan, T. and Lawrence, M.: Sensitivity of NO_x over the Indian Ocean to emissions from the surrounding continents and nonlinearities in atmospheric chemistry responses, Geophys. Res. Lett., 31, doi:10.1029/2004GL020210, 2004.

Lauer, A., Dameris, M., Richter, A., and Burrows, J. P.: Tropospheric NO_2 columns: a comparison between model and retrieved data from GOME measurements, Atmos. Chem. Phys., 2, 67–78, 2002, http://www.atmos-chem-phys.net/2/67/2002/.

Lawrence, M. and Crutzen, P.: Influence of NO_x emissions from ships on tropospheric photochemistry and climate, Nature, 402, 167–170, 1999.

Noxon, J.: Nitrogen dioxide in the stratosphere and tropsphere as measured by ground-based absoption spectroscopy, Science, 189, 547–549, 1975.

Olivier, J. and Berdowsky, J.: Global emission sources and sinks, in: The Climate System, edited by: Berdowski, J., Guicherit, R., and Heij, B., A. A. Balkema Publishers/Swets & Zeitlinger Publishers, Lisse, The Netherlands, pp. 33–77, 2001.

Olivier, J. G. J., van Aardenne, J. A., Dentener, F., Ganzeveld, L., and Peters, J. A. H. W.: Recent trends in global greenhouse gas emissions: regional trends and spatial distribution of key sources, in: Non-CO_2 Greenhouse Gases (NCGG-4), edited by: van Amstel, A., Millpress, Rotterdam, iSBN 90 5966 043 9, pp. 325–330, 2005.

Platt, U., Perner, D., and Pätz, H.: Simultaneous measurement of atmospheric CH_2O, O_3, and NO_2 by differential optical absorption, J. Geophys. Res., 84, 6329–6335, 1979.

Pozzer, A., Jöckel, P., Tost, H., Sander, R., Ganzeveld, L., Kerkweg, A., and Lelieveld, J.: Simulating organic species with the global atmospheric chemistry general circulation model ECHAM5/MESSy1: a comparison of model results with observations, Atmos. Chem. Phys., 7, 2527–2550, 2007, http://www.atmos-chem-phys.net/7/2527/2007/.

Richter, A. and Burrows, J.: Tropospheric NO_2 from GOME measurements, Adv. Space Res., 29, 1673–1683, 2002.

Richter, A., Eyring, V., Burrows, J., Bovensmann, H., Lauer, A., Sierk, B., and Crutzen, P.: Satellite measurements of NO_2 from international shipping emissions, Geophys. Res. Lett., 31, doi:10.1029/2004GL020822, 2004.

Song, C., Chen, G., Hanna, S., Crawford, J., and Davis, D.: Dispersion and chemical evolution of ship plumes in the marine boundary layer: Investigation of $O_3/NO_y/HO_x$ chemistry, J. Geophys. Res., 108, doi:10.1029/2002JD002216, 2003.

van Noije, T. P. C., Eskes, H. J., Dentener, F. J., Stevenson, D. S., Ellingsen, K., Schultz, M. G., Wild, O., Amann, M., Atherton, C. S., Bergmann, D. J., Bey, I., Boersma, K. F., Butler, T., Cofala, J., Drevet, J., Fiore, A. M., Gauss, M., Hauglustaine, D. A., Horowitz, L. W., Isaksen, I. S. A., Krol, M. C., Lamarque, J.-F., Lawrence, M. G., Martin, R. V., Montanaro, V., Müller, J.-F., Pitari, G., Prather, M. J., Pyle, J. A., Richter, A., Rodriguez, J. M., Savage, N. H., Strahan, S. E., Sudo, K., Szopa, S., and van Roozendael, M.: Multi-model ensemble simulations of tropospheric NO_2 compared with GOME retrievals for the year 2000, Atmos. Chem. Phys., 6, 2943–2979, 2006, http://www.atmos-chem-phys.net/6/2943/2006/.

Wang, C., Corbett, J., and Firestone, J.: Improving Spatial Representation of Global Ship Emissions Inventories, Environ. Sci. Technol., 42, 193–199, 2008.